Alternative Surface-Mounted Permanent Magnet Topology for Reducing Voltage and Torque Harmonics in Shaft Generators

Rak-Won Son and Ju Lee *

Posted Date: 21 April 2023

doi: 10.20944/preprints202304.0703.v1

Keywords: surface permanent magnet; modular pole; step-skew; induced voltage; torque pulsation; radial ventilation duct

Article

Alternative Surface-Mounted Permanent Magnet Topology for Reducing Voltage and Torque Harmonics in Shaft Generators

Rak-Won Son [1,2] and Ju Lee [2,*]

[1] Dept. of Electric Power Machinery Research, HD Hyundai Electric, Seongnam 13553, Korea; son.rakwon@hyundai-electric.com
[2] Dept. of Electrical Engineering, Hanyang University, Seoul 14763, Korea; julee@hanyang.ac.kr
* Correspondence: julee@hanyang.ac.kr; Tel.: +82-2-2220-0349

Abstract: Typically, a diesel generator on the merchant ship, composed of a wound rotor synchronous generator and a four-stroke diesel engine, supplies electrical power to various loads. Recently, shaft generators for merchant vessels are increasingly replacing diesel generators to reduce CO_2 emissions through fuel efficiency improvement. In particular, permanent magnet generators replace induction generators due to their high-efficiency characteristics at light loads. The surface-mounted permanent magnet can be a suitable rotor topology due to the relatively short constant power range. This generator can also operate as a motor according to the propulsion mode, so minimizing the harmonics of the induced voltage and the torque ripple is necessary. This paper proposes an alternative NdFeB magnet pole topology combined with the modular step-skewed rotor. The step-skewed rotor affects to reduce higher-order harmonics, and the modular pole reduces the permanent magnet assembly process and harmonics in voltage and torque. A 2-D finite element method is used to evaluate the harmonics of induced voltage and torque pulsation for the proposed topology. The topology shows harmonic minimization effect by comparing the characteristics of three flatted-bottom magnets. Compared to the tapered bread-loaf magnet, voltage harmonics to the 100th component are almost the same, and the torque ripple is reduced by more than 12% at the same residual flux density. The analysis method is verified by comparing test and analysis results for prototype machines with similar specifications.

Keywords: surface-mounted permanent magnet; modular pole; step-skew; induced voltage; torque pulsation; radial ventilation duct

1. Introduction

Conventional merchant ships have several diesel generators to supply electrical power for various devices, e.g., cranes and pumps. The required power and load fluctuation decide the combination of the number and rated power of the diesel generators. This kind of generator installed inside the hull is a power generation system that combines a four-stroke engine and a wound-field synchronous generator. Usually, synchronous generators have six to ten poles for the engine's rated speed range of 720 to 1,000 rpm. These generators operate at the same speed. An automatic voltage regulator controls the generator's terminal voltage at the same level in response to voltage and frequency fluctuations caused by load variation.

Meanwhile, the two-stroke engine is usually installed at the stern for ship propulsion and operates at less than 200 rpm. This engine shows a relatively high specific fuel oil consumption (SFOC) compared to the four-stroke engine. Utilizing this high SFOC characteristic, a shaft generator installed between the two-stroke engine and the propeller can be an alternative to partially eliminate the one or two diesel generators applied to large merchant ships. As a result, shaft generators have been widely used for merchant ships to enhance fuel efficiency and thus reduce CO_2 emissions. This kind of generator can also operate as a motor abided by ship operation mode. In generator mode, low voltage harmonic is the primary design requirement not to make additional harmonic losses in winding and core parts. While in motoring, low torque pulsation composed of cogging torque and

torque ripple is a critical design requirement to reduce acoustic noise and mechanical vibration. The application of permanent magnet synchronous generators, which show high-efficiency characteristics compared to induction machines, especially at light loads, has been increasing recently.

Ideal AC synchronous machines have pure sinusoidal air-gap flux density, making almost no voltage harmonics and torque pulsation in no-load and load operations. Several electromagnetic phenomena happen in real machines, e.g., magnetic saturation in electrical sheets, slot opening in the stator core, and non-sinusoidal air-gap flux density from the magneto-motive force in the rotor. These electromagnetic phenomena increase harmonics in air-gap flux density, which in turn deteriorates voltage and output torque waveforms. Magnetic saturation is inevitable in high-power rotating machines to reduce volume and weight. Especially in high-voltage rotating machines, a stator wire cross-section is almost rectangular to ensure enough dielectric and mechanical strength. In this case, the slot opening width is determined considering the current density and the corresponding heat dissipation performance. Therefore, in the actual design, one proper solution to reduce harmonics in voltage and torque is a design approach of making air-gap flux density more sinusoidal.

Due to their relatively short constant power range, many shaft generators can have surface-mounted permanent magnet (SPM) rotors. The SPM rotors have two design approaches to reduce voltage harmonics or torque pulsation by making quasi-sinusoidal air-gap magnetic flux density distribution. The former can be classified into four methods: Halbach array, magnet segmentation, magnet shaping, and modular pole. The Halbach array consists of several magnet pieces, and the magnetization directions of the magnet pieces are magnetized in different directions to make the air gap flux distribution sinusoidal. This quasi-sinusoidal flux distribution makes negligible cogging torque and almost sinusoidal voltage waveform, and the rotor rim is not essential due to self-shielding magnetization in small machines [1,2]. Still, there is a disadvantage, especially in large appliances, permanent magnets with various magnetization directions shall be assembled into one rotor pole piece or magnetized. Moreover, since it has to withstand the disturbance transmitted from the main engine and propeller, the rotor must have a sturdy rotor rim connected to the main shaft. The second method is magnet segmentation, meaning one pole has many permanent magnets with different widths [3]. This method positively affects air-gap space harmonics, cogging torque, and magnet loss decrease. Since permanent magnets of different widths must be magnetized and assembled, separate magnetizers for each permanent magnet and manufacturing facilities shall be furnished in a large multi-pole machine. In addition, since each permanent magnet is separated from the other, it is necessary to secure structural stability by constructing empty gaps with non-magnetic materials.

A usual method of magnet shaping is tapering. In this structure, the permanent magnet's thickness in the center of one pole is thicker than that of the edge [4–8]. As a result, the air gap length between the rotor and the stator core becomes non-uniform. This method is also very effective in making the air gap flux density sinusoidal. However, as intensive research was conducted on high-speed machines, arc or ring shapes were mainly studied to use permanent magnets efficiently. Another magnet shaping method is the addition of a third or higher harmonics to the permanent magnet shapes [9,10]. Fundamental flux density in the air gap can increase by the effect of the triploid harmonics on sinusoidal waveforms. Hence, the output torque increases, whereas the torque ripple also increases due to additional harmonics. The fourth way is by using a modular pole. This kind of pole has several magnets, which can be classified as a method of stacking multiple magnets in the radial direction [11,12] and arranging them in the radial direction [13]. Both ways show a significant effect in improving the quality of the air gap flux density. The skewed rotor or stator has several axial step-core with a separation distance of usually one stator slot angle [14–18]. This method effectively cancels higher harmonics, which operate as a low-pass filter. While continuous skew is usually applied to induction machines, step- skew can easily be used in SPM machines using separated magnets in the axial direction.

Small electric motors were targeted in previous papers, so most research focused on arc-shaped permanent magnets. This shape is not easy to handle in magnetization and assembly processes due

Preprints (www.preprints.org) | NOT PEER-REVIEWED | Posted: 21 April 2023 doi:10.20944/preprints202304.0703.v1

to the pointed end of a large permanent magnet having a width of 200 mm or more. In some designs, which are Halbach array, magnet segmentation, and modular pole, many permanent magnets are arranged in a complex shape to reduce air gap flux harmonics. Also, it is difficult to find research results that consider all harmonics of voltage, cogging torque at no load, and torque ripple at load operation simultaneously.

This paper proposes an alternative SPM topology incorporating a modular step-skewed rotor to reduce harmonics in voltage and torque. Considering the multi-pole structure, permanent magnets with two different shapes and residual magnetic flux densities constitute one pole, making the air gap quasi-sinusoidal harmonics. The step-skewed rotor was applied to increase the effect of reducing high-order harmonics. The 2-D finite element method is used to evaluate a low-speed generator's induced voltage and torque pulsation of both cogging torque and torque ripple. The comparative analysis shows that induced voltage harmonics are almost the same. The torque ripple can be reduced by more than 12% at the same residual flux density compared to the tapered bread-loaf magnet. Since both permanent magnets have a flat bottom, manufacturing and handling are easy.

2. Proposed NdFeB Magnet Configuration

A bread-loaf magnet in Figure 2 has an excellent effect on making quasi-sinusoidal flux density in the air gap, especially in low-speed large synchronous machines. Because of these machines' relatively big diameter-to-axial length ratio, the magnet can have an almost flat bottom outside the rotor rim. This kind of magnet also can reduce magnet bulk at the same magnetic loading and causes the rotor assembly manufacturing process more efficient due to its flat bottom. Table 1 represents the specification of a prototype machine together with the bread-loaf magnet. Based on the 2-D finite element (FE) model in Table I, Figure 1 shows air-gap radial flux density on no-load for three kinds of magnets; conventional bread-loaf magnet, tapered bread-loaf magnet, and proposed modular magnet.

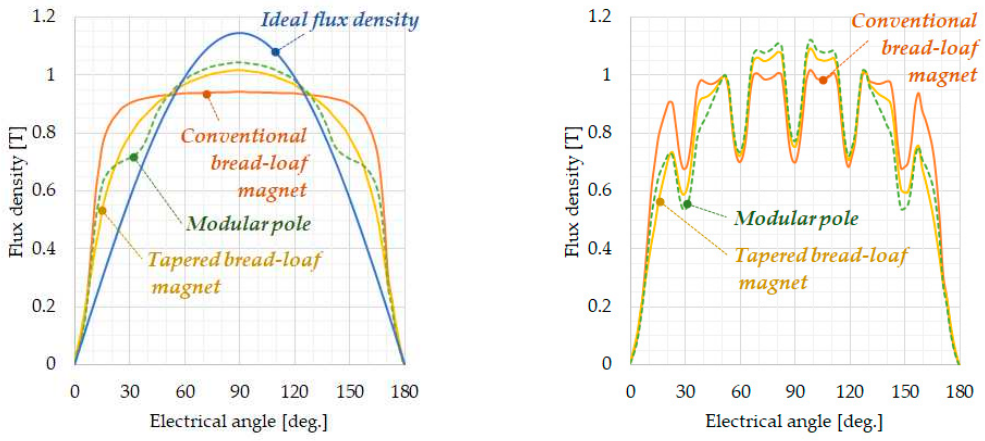

Figure 1. Air-gap radial flux density on no-load for one pole: (**a**) Flux density filled with magnetic material in slot opening; (**b**) Flux density with non-magnetic material in slot opening.

Preprints (www.preprints.org) | NOT PEER-REVIEWED | Posted: 21 April 2023 doi:10.20944/preprints202304.0703.v1

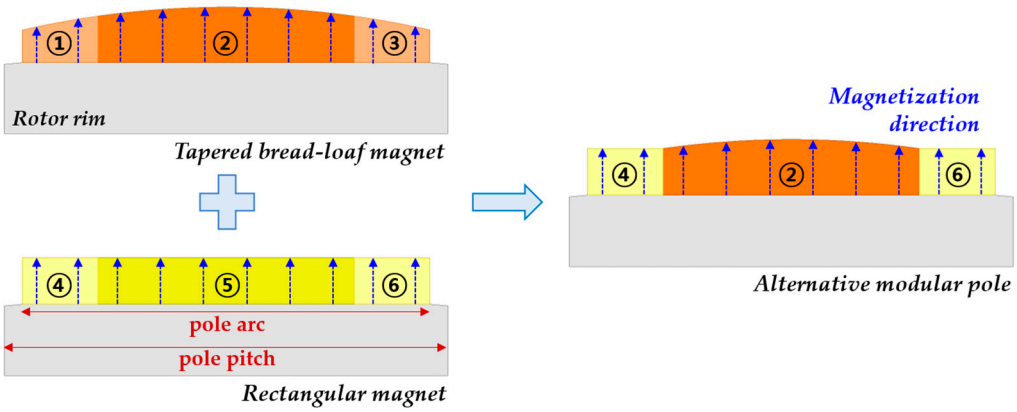

Figure 2. A modular pole topology.

Table 1. Specification of a prototype machine.

Design variable	Unit	Specifications
Rated power	kVA	2,100
Rated speed	rpm	65
Number of phases	-	3
Number of poles	-	32
Number of slots	-	192
Stator outer diameter	mm	2,310
Stator inner diameter	mm	2,000
Minimum air-gap length	mm	6
Maximum magnet height	mm	24
Rotor rim height	mm	50
Core length except radial ducts	mm	900
Number of core packet	EA	20
Core material	-	50PN400
Skew angle	no. of slot	One slot pitch on rotor

2.1. Proposed magnet design approach

The tapered bread-loaf magnet and the proposed modular magnet have a maximum air-gap length of 12mm. So minimum to maximum air-gap length ratio is 2. All magnet pole has a pole arc ratio of 0.89, defined as the ratio of pole arc to pole pitch as in Figure 2. The 2-D FE model includes magnetic saturation effect in electrical sheets using 50PN400 material data. The induced voltage at no-load is set as 500V by adjusting residual flux density. The three air-gap flux densities appear symmetrical, centered at 90 degrees, and smooth waveform about the pole center due to the bilateral symmetry-shaped magnet and no armature reaction. As the slot opening is filled with magnetic material, which means the same as the core, a conventional bread-loaf magnet shows almost isosceles trapezoidal flux density in ideal conditions. Under this condition, the no-load terminal voltage is reduced by more than 3% for all three models due to the leakage flux passing through the slot opening. The torque ripple increases due to the reduced reluctance in the slot opening. When the slot opening effect is considered, as in Figure 1b, the air-gap flux waveform is distorted and shows higher harmonics due to the slotting effect from the stator core.

Against ideal flux density, a conventional bread-loaf magnet shows that unnecessary magnetic flux happens in the magnet edge. There are two options: increasing flux in the pole center or decreasing flux in the pole edge by modifying pole shape; A tapered bread-loaf magnet, which also means irregular air-gap length, is a very effective rotor topology in making air-gap flux density more sinusoidal as in Figure 1a and reducing eddy-current loss inside the magnet. However, this magnet shape has significant drawbacks: reduced mechanical stability and increased demagnetization

Preprints (www.preprints.org) | NOT PEER-REVIEWED | Posted: 21 April 2023 doi:10.20944/preprints202304.0703.v1

possibility due to the relatively thin edge parts. Large magnets must be divided and used for manufacturing safety and uniform magnetization.

This paper suggests an alternative pole topology to reduce these drawbacks, as in Figure 2. An idea of the modular pole topology comes from a composite structure of a center magnet (2) from the tapered bread-loaf magnet and edge magnets (4, 6) from the rectangular magnet. In other words, one pole has two kinds of magnet: one tapered bread-loaf magnet (2) is located in the center of the pole with relatively high remanence to satisfy the required induced voltage, and the location of two rectangular-shaped magnets (4, 6) is outside of the center magnet. These edge magnets shall have relatively low residual flux density to make air-gap flux density more sinusoidal. Two-edge magnets can have any magnet, such as ferrite, alnico, SmCo, and NdFeB. However, in a high-powered rotating machine, the NdFeB magnet is proper due to the high coercivity to protect the magnet from partial demagnetization. The magnetization direction of this magnet is parallel, which means vertical direction to the magnet bottom, which makes the magnetization process easy.

2.2. Step-skewed rotor

In a large synchronous machine, a long axial core length over 300mm makes it easy to have a step-skew over three steps or more. Figure 3 shows one axial module of the machine for two poles with five step-skewed magnets. The pole arc ratio is 0.8, and the maximum air-gap length is 12mm in this figure. The magnet width ratio between the center magnet and edge magnets is 3.5. A modular step-skewed rotor assembly consists of SPMs and rotor rims, as shown in Figure 2. Two modules are axial symmetrical in the shape of an inverted V. This magnetically balanced rotor topology can reduce the axial force with the help of radial ventilation ducts. Several radial ventilation ducts are located between core packets to increase cooling performance, especially in the winding. These radial ventilation ducts have an effect on decreasing inter-pole leakage flux owing to a relatively longer distance than air-gap in this design. A kind of magnet cover is essential to protect a bundle of magnets in both the manufacturing process in the shipyard and load operation, which is excepted in Figure 3 to make the design approach simple. The rotor rim is connected to the intermediate shaft through additional shaft flanges. The stator core has segmented structures due to the length limit of non-oriented electrical sheets. In this design, the maximum probable number of the segmented stator core in the circumferential direction is 8.

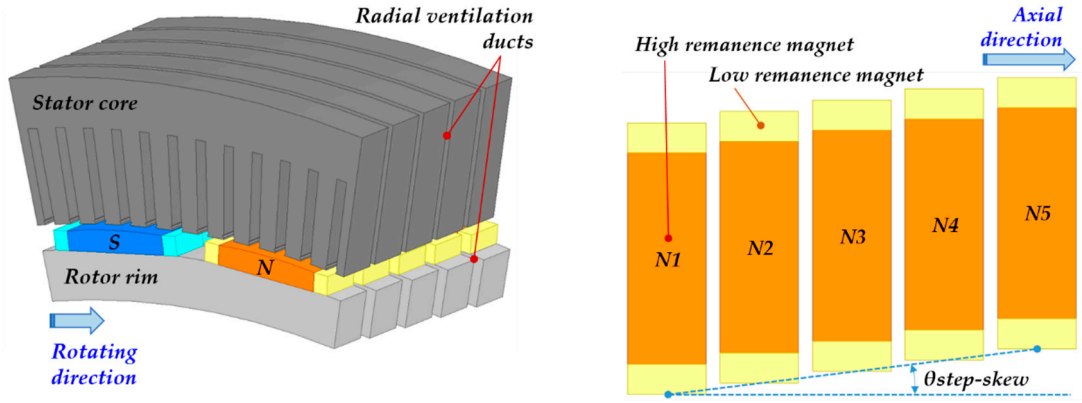

(**a**) (**b**)

Figure 3. Modular pole and stator core: (**a**) Rotor and stator core with radial ventilation ducts; (**b**) Step-skewed magnet arrangement with the modular pole.

The shape of the stator winding is rectangular, including several layer insulations, to withstand high-voltage with enough mechanical strength and get enough dielectric strength and partial discharge characteristics. As the width of the slot opening shall be enough to assemble or insert the stator winding into the stator core, cogging torque substantially occurs with the additional effect of integer slot-distributed winding.

Preprints (www.preprints.org) | NOT PEER-REVIEWED | Posted: 21 April 2023 doi:10.20944/preprints202304.0703.v1

The cogging torque occurs by the interaction between magneto-motive forces from permanent magnets and reluctance variation inside the stator bore, in brief, air-gap permeance variation. The cogging torque can be easily observed in no-load operation, and a modular step-skewed rotor is one of the solutions to reduce or eliminate cogging torque. To cancel harmonics by using step-skew, one period of harmonics shall be overlapped. It means the period of step-skew shall be determined as the least common multiple (LCM) of the number of poles (P) and slots (S). So, the total skew angle for (n)-step-skew in Figure 3b can be calculated as (1).

$$\theta_{step-skew} = \frac{360°}{LCM(P,Q)} \cdot \frac{n-1}{n} \quad (1)$$

The prototype machine has 32 poles and 192 slots. Thus the skew angle between each core packet is 0.375 degrees.

3. Characteristic Comparison of Voltage and Torque

A 2-D FE model used in this paper on one pole reduces solving time than a 3-D model. Time stepping method with a transient solver attempts to evaluate time harmonics in voltage and torque. In this case, the time step and mesh size shall be small enough to get a precise calculation result in a skewed rotor; the number of sampling shall be over 30 to decide the time step, and the number of mesh layers in the air-gap is over 4. The superposition method for each skewed rotor is suitable for considering the skew effect. An ideal sinusoidal current source is applied to get its machine's harmonics.

3.1. Cogging torque minimization with step-skew

Figure 4 shows the magnitude of cogging torque by skew angle variation from 2 to 10-step rotor. The no-skewed rotor's magnitude is 13.26kNm, which means 4.4% of the rated torque. This ratio means tremendous cogging torque and can cause high vibration in no-load operation. The cogging torque phase overlaps at a grayed dot point in the skew angle of 1.0 p.u. When the number of skews is over 4, the cogging torque is below 0.1% of the rated torque. As the number of skew increases further, the magnitude of cogging torque eventually almost disappears. It is also found that as the number of skew increases, cogging torque variation according to skew angle decreases; this means that using a high number of skews can solve increased cogging torque from manufacturing tolerance.

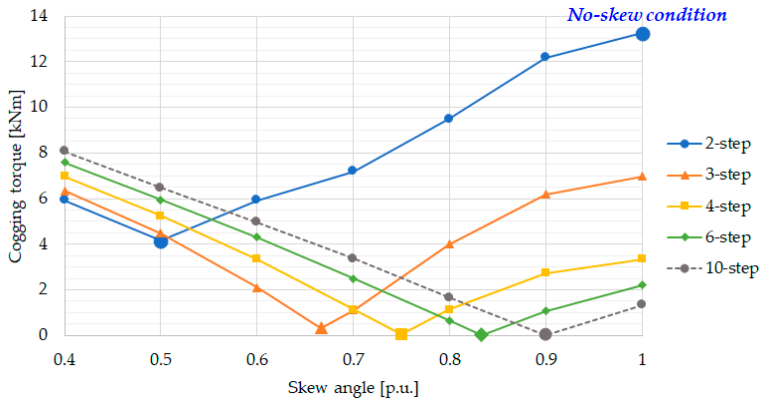

Figure 4. Cogging torque magnitude by the number of step-skew.

In a no-skewed rotor, the main component of cogging torque is the 12th harmonic in an electrical period, shown in Figure 5. In 2-step-skew, the 24th harmonic is dominant due to eliminated 12th harmonic. When the number of step increase over 3, it can be seen that the cogging torque almost disappears, as shown in Figure 4. Of course, the phase and magnitude of the cogging torque may fluctuate somewhat due to the axial flux effect, including the end-leakage flux. This effect is expected not to be significant due to minimized leakage flux by the radial ventilation ducts.

Preprints (www.preprints.org) | NOT PEER-REVIEWED | Posted: 21 April 2023 doi:10.20944/preprints202304.0703.v1

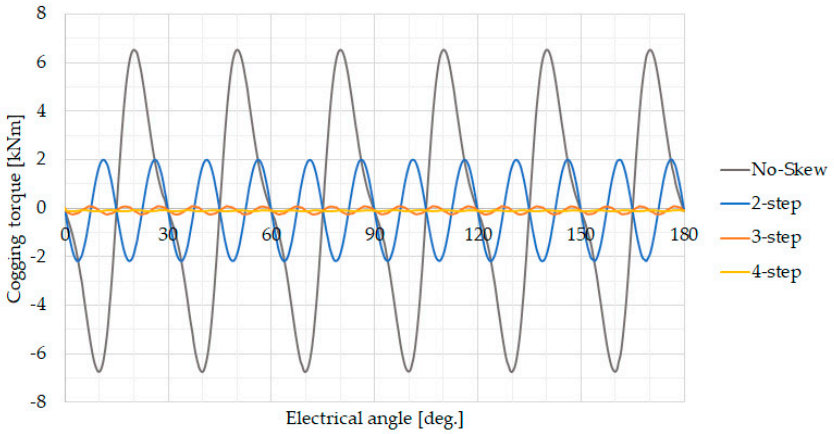

Figure 5. Cogging torque waveform by the number of step-skew.

3.2. Harmonic minimization in voltage and torque ripple

2-D FE models with a bread-loaf type magnet are used to find a proper pole-arc ratio that minimizes both the voltage harmonics and torque ripple. The following assumptions are applied as preconditions to simplify the design approach. First, the dimensions of the stator winding, stator core, and rotor core are the same. Second, the magnet thickness is fixed as four times the air-gap length because the thickness of the magnet is a critical design variable to decide the degree of demagnetization, especially in SPM topology. In contrast, the remanence of the magnet is adjusted to have the same flux linkage in the stator winding for rated operation. Although the harmonic characteristics of the induced voltage can be evaluated as individual components, Equation (2) is used here to comprehensively consider from first to the 100th harmonic component. Torque ripple can be defined in various ways, and it is defined here as the deviation of the maximum and minimum torque from the average torque, as shown in Equation (3).

$$THD = \sqrt{\sum_{n=2}^{100} \left(\frac{U_n}{U_1}\right)^2} \tag{2}$$

$$T_{ripple} = \frac{T_{maximum} - T_{minimum}}{T_{average}} \tag{3}$$

Figure 6 shows the harmonics of the induced voltage and the torque ripple according to the change in pole arc ratio. It can be confirmed that the harmonic component significantly decreases according to the application of the skew. Even if the skew is applied, the fluctuation range of the harmonic component is extensive according to the pole arc ratio, e.g., torque ripple has a 3.4 times difference. In this model, an important matter is that there is no pole arc ratio value where voltage harmonic and torque ripple have minimum simultaneously; the optimal pole arc ratio to reduce harmonics is 0.80 for back-EMF and 0.90 for torque ripple.

Preprints (www.preprints.org) | NOT PEER-REVIEWED | Posted: 21 April 2023 doi:10.20944/preprints202304.0703.v1

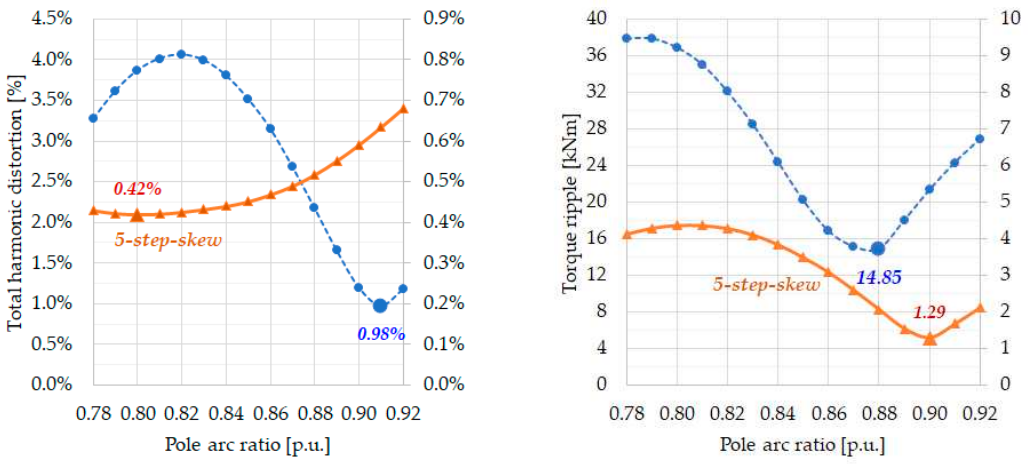

(**a**) (**b**)

Figure 6. Harmonic characteristics of conventional bread-loaf magnet with or without 5-step-skew: (**a**) Total harmonic distortion in induced voltage; (**b**) Torque ripple.

Table 2 shows the FE analysis results of pole-arc ratio and maximum air-gap length variation, that is, magnet width ratio, for the proposed modular pole. At this time, the relative permeability of the magnet is 1.05, and the remanence of edge magnets is 1.0T; an N28UH grade magnet has a residual flux density of 1.0T at 80 degrees. Current phase angle control is excluded; the phase angle is 0 degrees. Each point of minimized THD and torque ripple are underlined for each pole arc ratio. From the analysis result, as the maximum air-gap length increases, the remanence of the main magnet for the same induced voltage increases due to the fixed remanence of the edge magnet. Even when the pole arc ratio increase, there is no significant difference in the THD value of the induced voltage, indicating that the effect of suppressing harmonic components is powerful. The torque ripple is minimized to the level of an induction motor with 0.35% of the rated torque at a pole arc ratio of 0.90, the same as the conventional bread-loaf magnet.

Table 2. Harmonic characteristics with different pole arc ratios.

Pole arc ratio	Maximum air-gap length	Remanence of center magnet	Remanence of edge magnet	THD of induced voltage	Torque ripple
p.u.	mm	T	T	%	%
0.80	7	1.267	1.000	0.34	1.18
	8	1.297	1.000	0.33	1.10
	9	1.326	1.000	0.35	1.16
0.89	9	1.255	1.000	0.31	0.48
	10	1.275	1.000	0.31	0.43
	11	1.294	1.000	0.34	0.42
0.90	9	1.250	1.000	0.35	0.59
	10	1.269	1.000	0.35	0.51
	11	1.287	1.000	0.37	0.41
	12	1.305	1.000	0.40	0.35
	13	1.322	1.000	0.43	0.36

3.3. Characteristic comparison of four different magnet designs

It is essential to discover how effectively the suggested design improved harmonic characteristics. The shape of four magnets are presented in Figure 7. Generally, the bread-loaf magnet in (a) and (b) is advantageous in generating a sinusoidal air gap magnetic flux density, so it is often used in the SPM rotor. The design (c) represents a rectangular-shaped magnet and is widely applied

Preprints (www.preprints.org) | NOT PEER-REVIEWED | Posted: 21 April 2023 doi:10.20944/preprints202304.0703.v1

to interior permanent magnet synchronous motors because it is easy to magnetize and assemble. All magnets have a pole arc ratio of 0.9 for comparison.

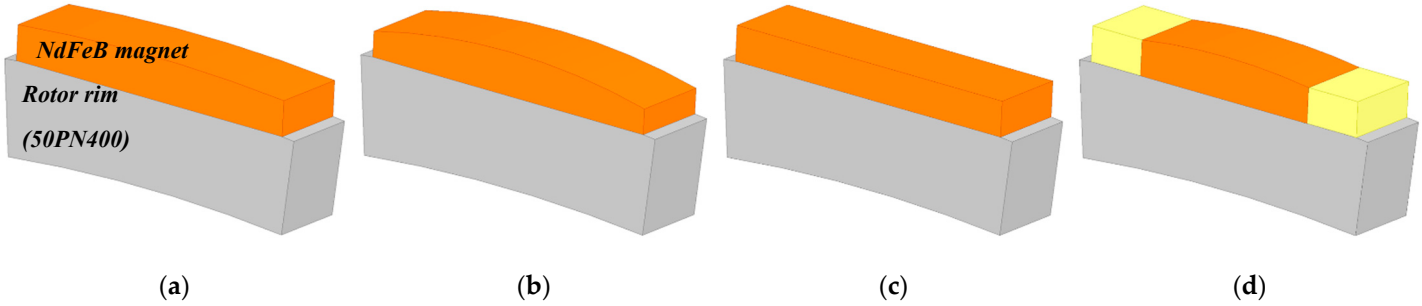

Figure 7. Four different magnet designs for one pole segment used in the performance comparison: (**a**) Conventional bread-loaf magnet; (**b**) Tapered bread-loaf magnet; (**c**) Rectangular-shaped magnet; (**d**) Proposed modular pole.

The electromagnetic torque characteristics with the change of the current phase angle are summarized in Figure 8. Since operating at the maximum torque point on rated current is usually an efficient driving method, we first tried to find the maximum torque point. It can be seen that there is no significant difference in electromagnetic torque under the same pole arc ratio and magnet depth conditions. The non-uniform magnet depth of designs (b) and (d) shows increased electromagnetic torque owing to reluctance torque because of a slight difference between d-axis and q-axis inductances. It can also be seen that the phase angle of the current generating the maximum torque shifts by 2 degrees instead of zero due to the different air gap lengths and the relative permeability of 1.05. As the current phase angle increases, the torque ripple shows an increasing or decreasing pattern according to the magnet shape.

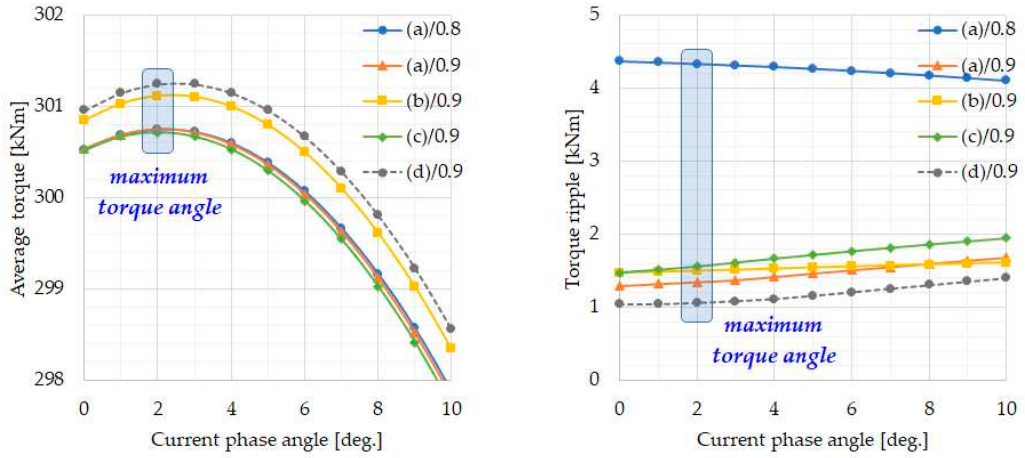

Figure 8. Electromagnetic torque characteristic with different current phase angle.

Figure 9 shows the electromagnetic torque waveform based on the electrical angle of 180 degrees for each rotor design at the current phase angle of 2 degrees, where the maximum torque occurs. When the pole arc ratio is 0.8, the 6th and 12th harmonics dominate, but when the pole arc ratio is 0.9, the 12th harmonic component becomes the main component. In addition, design (d) has the most considerable average torque and minimizes the torque ripple.

Table 3 represents the summarized characteristics of induced voltage and torque ripple for the four designs in Figure 7. Compared to a tapered bread-loaf magnet with a pole ratio of 0.90, the proposed modular pole with a pole arc ratio of 0.89 has almost the same induced voltage harmonics as underlined. Torque ripple was reduced by 12% from 0.49% to 0.43%. Even when the pole arc ratio

Preprints (www.preprints.org) | NOT PEER-REVIEWED | Posted: 21 April 2023 doi:10.20944/preprints202304.0703.v1

is 0.90 in the proposed modular pole, the torque ripple is 0.35%, the smallest value among the four-rotor topologies. From this result, the proposed design (d) minimizes the harmonic components of induced voltage and torque ripple more effectively than rotor (b) by adjusting the pole arc ratio and maximum gap length.

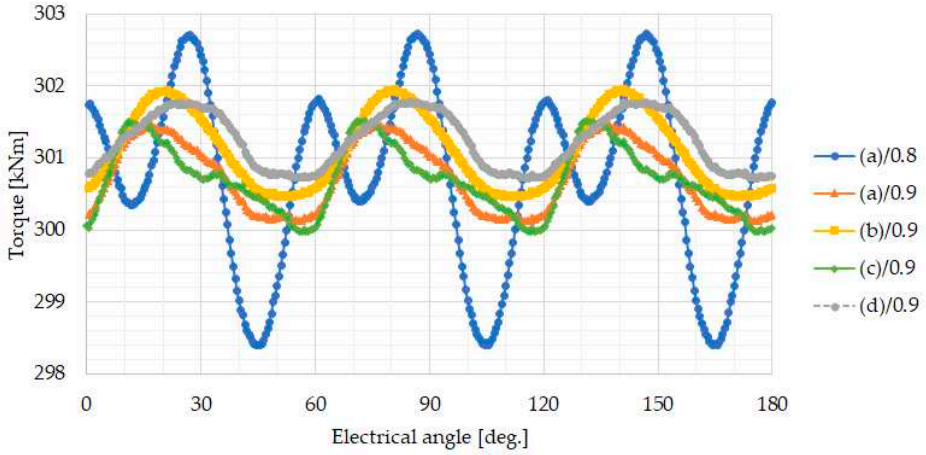

Figure 9. Electromagnetic torque waveform of five different magnet designs.

Table 3. Voltage harmonics and torque characteristics for different rotor topologies.

Rotor topology	Pole arc ratio	Maximum air-gap length	Remanence of center magnet	THD of induced voltage	Average torque	Torque ripple
	p.u.	mm	T	%	kNm	%
Conventional bread-loaf magnet	0.90	6	1.189	0.59	300.5	0.43
Tapered bread-loaf magnet	0.90	12	1.273	0.29	300.8	0.49
Rectangular magnet	0.90	6	1.380	0.74	300.5	0.49
Proposed modular pole	0.89	10	1.275	0.31	300.8	0.43
	0.90	12	1.305	0.40	301.0	0.35

4. Model validation of finite element method

A no-load test was conducted on an already manufactured prototype machine with similar specifications. The test result was compared to the 2-D FE analysis result to verify the accuracy of the 2-D FE analysis method used for a machine in Table 1. The 2-D analysis condition is the same, e.g., boundary condition and mesh quality.

The tested machine is a three-phase, 2MW, 500V, 24-pole permanent magnet synchronous generator for ship propulsion systems. The height of the frame, excluding the upper heat exchanger, is 2.9m, and the width is 3.1m. As shown in Figure 10a, a terminal box is installed on the left side of the frame, and a heat exchanger with fan motors is located on the top of the frame to generate sufficient airflow. Figure 10b shows the assembled stator core and winding assembly before vacuum impregnation. The stator and rotor cores consist of non-oriented electrical steel, 50PN400. Due to the electrical steel sheet's dimensional limitations, several separated cores were assembled into the whole core. The stator winding was made in rectangular copper wire to reduce partial discharge and respond to the inverter's instantaneous voltage. Compared to wound rotor synchronous machines, NdFeB magnet rotors minimizes the loss generated in the rotor part. Since heat generation due to rotor loss is minimized, power density can be improved.

In the no-load test, the dynamo drives the generator at the rated speed of 56rpm, and the voltage is measured from stator terminals. Since the stator windings are open, there is no armature reaction due to stator magneto-motive force. Therefore, measuring the terminal voltage from the magneto-motive force of the permanent magnet is possible. It is the first test to measure whether the rotor is

Preprints (www.preprints.org) | NOT PEER-REVIEWED | Posted: 21 April 2023 doi:10.20944/preprints202304.0703.v1

appropriately designed to meet the required specifications. From this test, we can also measure iron loss, mechanical loss, and noise. The line-to-line voltage waveform was measured with an oscilloscope. Harmonic components and THD up to the 100th harmonic according to IEC 60034-1 can be calculated by Fourier transform. According to this standard, the THD value of the terminal voltage during no-load operation must be less than 5%. The test and analysis results of no-load voltage are presented together in Figure 11.

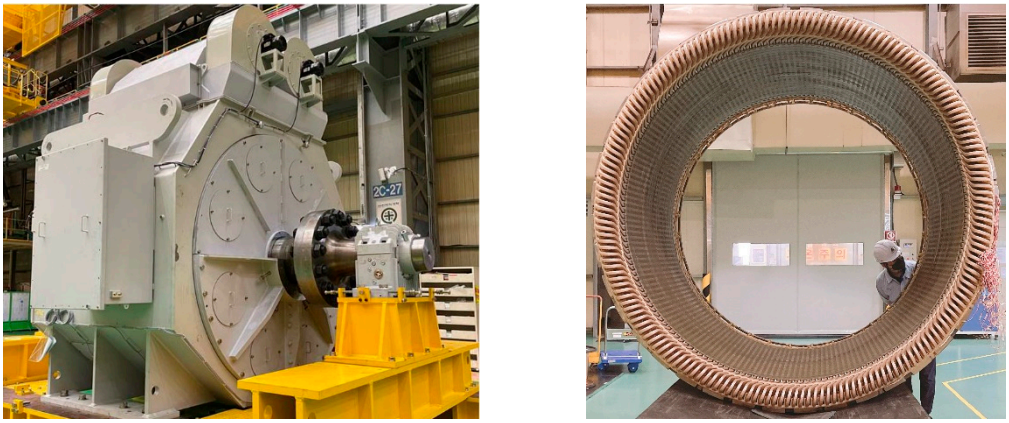

(**a**) (**b**)

Figure 10. 2MW permanent magnet synchronous machine for ship propulsion systems: (**a**) External appearance; (**b**) Stator core and winding assembly.

The fundamental deviation between the test and analysis is less than 2%. Figure 11 is modified so that the fundamental wave component is 100%. The seventh harmonics occurs prominently, and its magnitude is about 0.5% to the fundamental and can be confirmed to be small enough to be ignored. In addition, the THD analysis result from the fundamental to the 100th order is 0.58%, and the deviation is less than 6% compared to the average value of 0.55% of the test results. Hence, voltage harmonics satisfy the IEC 60034-1 rule. The accuracy of the 2-D FE model has been verified.

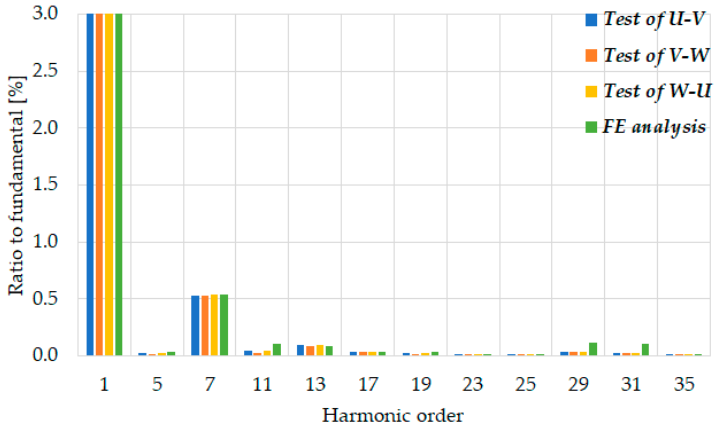

Figure 11. Induced voltage harmonics from analysis and test results.

5. Conclusions

This research proposes a modular pole topology to reduce voltage harmonics and torque pulsation at the same time. This topology uses a step-skewed rotor to minimize cogging torque to a negligible level. In addition, the combined magnet shape composed of a tapered bread-loaf magnet and two rectangular magnets minimizes the induced voltage and torque pulsation harmonics. The harmonic minimization effect was verified by comparing the characteristics of the three topologies

with flat-bottom. The 2-D FE analysis method was verified by comparing test and analysis results on similar prototype machines. The topology proposed in this paper will effectively reduce voltage harmonics and torque pulsation of multipole rotors. In the following research, we will find out the voltage harmonics and torque pulsation fluctuations based on the 3-D FE model, considering the fringing and leakage flux effect in the axial direction.

References

1. Zhu, Z.Q.; Shen, Y. Investigation of permanent magnet brushless machines having unequal-magnet height pole. *IEEE Trans. Magn.* **2012**, *48*, 4815-4830. [10.1109/TMAG.2012.2202398]
2. Zhu, Z.Q.; Howe, D. Halbach permanent magnet machines and applications: a review. *IEE Proc.-Elect. Power Appl*. **2001**, *148*, 299-308. [10.1049/ip-epa:20010479]
3. Chaithongsuk, S.; Takorabet, N.; Meibody-Tabar, F. On the use of pulse width modulation method for the elimination of flux density harmonics in the air-gap of surface PM motors. *IEEE Trans. Magn*. **2009**, *45*, 1736-1739 [10.1109/TMAG.2009.2012801]
4. Li, Y.; Xing, J.; Wang, T.; Lu, Y. Programmable design of magnet shape for permanent-magnet synchronous motors with sinusoidal back EMF waveforms. *IEEE Trans. Magn*. **2008**, *44*, 2163-2167 [10.1109/TMAG.2008.2000750]
5. Hsieh, M.F.; Hsu, Y.S. An investigation on influence of magnet arc shaping upon back electromotive force waveforms for design of permanent-magnet brushless motors. *IEEE Trans. Magn*. **2005**, *41*, 3949-3951 [10.1109/TMAG.2005.854975]
6. Zheng, P.; Jing, Z.; Jianqun, H.; Jie, W.; Zhiyuan, Y.; Ranran, L. Optimization of the magnetic pole shape of a permanent-magnet synchronous motor. *IEEE Trans. Magn*. **2007**, *43*, 2531-2533 [10.1109/TMAG.2007.893631]
7. Tavana, N.R.; Shoulaie, A. Analysis and design of magnetic pole shape in linear permanent-magnet machine. *IEEE Trans. Magn*. **2010**, *46*, 1000-1006 [10.1109/TMAG.2009.2037951]
8. Laskaris, K.I.; Kladas, A.G. Permanent-magnet shape optimization effects on synchronous motor performance. *IEEE Trans. Ind. Elect*. **2011**, *58*, 3776–3783 [10.1109/TIE.2010.2093481]
9. Zhu, Z.Q.; Wang, K.; Ombach, G. Optimal magnet shaping with third order harmonic for maximum torque in brushless AC machines. *IET Int. Conf. Power Elect*. **2012**, 1-6 [10.1049/cp.2012.0275]
10. Wang, K.; Gu, Z.Y.; Zhu, Z.Q.; Wu, Z.Z. Optimum injected harmonics into magnet shape in multiphase surface-mounted PM machine for maximum output torque. *IEEE Trans. Ind. Elect*. **2017**, *64*, 4434-4443 [10.1109/TIE.2017.2669888]
11. Ree, J.D.L.; Boules, N. Magnet shaping to reduce induced voltage harmonics in PM machines with surface mounted magnets. *IEEE Trans. Energy Convers*. **1991**, *6*, 155-161 [10.1109/60.73802]
12. Dubois, M.R.; Mailloux, G. Analytical calculation of no-load voltage waveforms in machines based on permanent-magnet volume integration. *IEEE Trans. Magn*. **2008**, *44*, 581-589 [10.1109/TMAG.2008.918920]
13. Isfahani, A.H.; Vaez-Zadeh, S.; Rahmanm M.A. Using modular poles for shape optimization of flux density distribution in permanent-magnet machines. *IEEE Trans. Magn*. **2008**, *44*, 2009-2015 [10.1109/TMAG.2008.922781]
14. Hwang, S.; Lieu, D.K. Design techniques for reduction of reluctance torque in brushless permanent magnet motors. *IEEE Trans. Magn*. **1994**, *30*, 4287-4289 [10.1109/20.334063]
15. Islam, M.S.; Shrestha, A.; Islam, M. Performance comparison of step skew in interior and surface-mount permanent magnet machines. *IEEE Energy Conves*. **2021**. [10.1109/ECCE47101.2021.9595964]
16. Ocak, O.; Aydin, M. An innovative semi-FEA based, variable magnet-step-skew to minimize cogging torque and torque pulsations in permanent magnet synchronous motors, *IEEE Access*. **2020**, 8, 210775-210783 [10.1109/ACCESS.2020.3038340]
17. Nam, D.W.; Lee, K.B.; Pyo, H.J.; Jeong, M.J.; Yang, S.H.; Kim, W.H.; Jang, H.K. A study on core skew considering manufacturability of double-layer spoke-type PMSM. *Energies*. **2021**. *14*, 610 [10.3390/en14030610]
18. Jiang, J.W.; Bilgin, B.; Yang, Y.; Sathyan, A.; Dadkhah, H.; Emadi, A. Rotor skew pattern design and optimisation for cogging torque reduction. *IET Elect. Syst. Transp*. **2016**, *6*, 126-135 [10.1049/iet-est.2015.0021]

disclaim responsibility for any injury to people or property resulting from any ideas, methods, instructions or products referred to in the content.